Topological Hall effect in thin films of the Heisenberg ferromagnet EuO

Y. Ohuchi,[1] Y. Kozuka,[1,*] M. Uchida,[1] K. Ueno,[2] A. Tsukazaki,[3,4] and M. Kawasaki[1,5]

[1]*Department of Applied Physics and Quantum-Phase Electronics Center (QPEC), University of Tokyo, Tokyo 113-8656, Japan*

[2]*Department of Basic Science, University of Tokyo, Tokyo 153-8902, Japan*

[3]*Institute for Materials Research, Tohoku University, Sendai 980-8577, Japan*

[4]*PRESTO, Japan Science and Technology Agency (JST), Tokyo 102-0075, Japan*

[5]*RIKEN Center for Emergent Matter Science (CEMS), Wako, Saitama 351-0198, Japan*

(Received 28 November 2014; revised manuscript received 19 May 2015; published 8 June 2015)

We report on the topological Hall effect (THE) in centrosymmetric EuO thin films. This THE signal persists down to the lowest temperature in the metallic region below 50 K for the films thinner than 200 nm. The signal rapidly disappears by tilting the applied magnetic field from surface normal, suggestive of noncoplanar spin configuration such as two-dimensional skyrmions. This observation possibly substantiates the theoretical proposal of magnetic skyrmions in 2D Heisenberg ferromagnets in marked contrast to better established $B20$-type chiral helimagnets.

DOI: 10.1103/PhysRevB.91.245115 PACS number(s): 72.15.Gd, 72.25.Dc, 75.47.Lx

Magnetic skyrmion is a topological spin texture, where nontrivial integer topological charge arises from its noncoplanar swirling spin configuration [1]. While the formation of skyrmions in chiral magnets has long been theoretically discussed [2] it is only recently that the magnetic skyrmions have been experimentally confirmed unambiguously in $B20$-type metallic helimagnets such as MnSi, $Fe_{0.5}Co_{0.5}Si$, and FeGe [3–5]. This class of compounds possesses a chiral crystal structure, which stabilizes magnetic skyrmions with an aid of Dzyaloshinskii-Moriya (DM) interaction under a magnetic field.

Magnetic skyrmions are also explored in other materials without involving the DM interaction. Centrosymmetric cubic $SrFe_{1-x}Co_xO_3$, for example, exhibits various helimagnetic phases, and the formation of magnetic skyrmions is proposed under magnetic field based on topological Hall effect (THE), possibly originating from the magnetic frustration [6,7]. As another mechanism, magnetodipolar interactions in easy-axis ferromagnetic thin films are known to give rise to the magnetic bubbles, which is topologically isomorphic with skyrmions [1]. Experimentally, Lorentz transmission electron microscopy clearly visualizes the magnetic bubble phase in M-type ferrite thin films [8].

We have pursued a topologically nontrivial magnetic structure in ferromagnetic EuO thin films [9,10], which is one of the well-studied ferromagnetic semiconductors with a band gap of ∼1.12 eV and a ferromagnetic transition temperature T_C of ∼70 K [11]. EuO has a small magnetic crystalline anisotropy constant $K_1 = -4.36 \times 10^{-2}$ J/cm^3 at 2 K because of the cubic and centrosymmetric crystal structure (rocksalt type) as well as zero angular momentum ($L = 0$) of localized $4f$ [7] spins at Eu^{2+} sites [12]. So far, no peculiar magnetic configuration has been reported other than simple ferromagnetic structure. Therefore, within the context of the aforementioned skyrmion materials, a nontrivial spin configuration is not expected to appear in EuO.

In this paper, we experimentally show formation of nontrivial magnetic structure in oxygen deficient EuO thin films by THE. This observation is surprising since EuO possesses neither structural nor magnetic properties which are fulfilled in many of the skyrmion materials. Nevertheless, the formation of skyrmions, or other topologically nontrivial spin structures, is well supported by the sensitive response of THE to the tilt of magnetic field, indicating instability to in-plane magnetic field as a typical response of two-dimensional (2D) magnetic skyrmions. The THE signal is also suppressed for the films with the thickness above 200 nm. All these facts show that this magnetic structure is thought to be formed in EuO thin films as a result of two dimensionality in this isotropic spin system.

EuO epitaxial films were grown on $YAlO_3$ (110) substrates by pulsed laser deposition at 300 °C using a Eu metal target under 1×10^{-5} Torr of Ar gas containing 1% O_2. We used KrF excimer laser pulses for the deposition at a repetition rate of 15 Hz. The details of the other growth conditions are described in Ref. [9]. The in-plane lattice constants of EuO thin films were investigated by reciprocal space mapping. We found that the crystal is relaxed to give little magnetoelastic anisotropy in EuO thin films, which is consistent with previous reports on magnetic properties of EuO films grown on $YAlO_3$ substrates [9,13]. We fabricated EuO films with various thicknesses (t = 23, 50, 73, 150, and 230 nm) covered with about 5-nm amorphous Al_2O_3 capping layers deposited *in situ* in order to avoid oxidization of Eu^{2+} in air. Film thickness was confirmed by x-ray reflectivity measurement except for the thickest sample (t = 230 nm), for which we used a stylus profiler. Films were patterned into Hall bars by photolithography (100 μm wide × 500 μm long) and Ar ion milling for transport measurements with a current density of 5.6×10^6 A/m^2. The Hall resistivity was analyzed by antisymmetrizing the raw Hall resistivity data (ρ_{xy}^{raw}) to exclude the contribution from longitudinal magnetoresistance as $\rho_{xy}(B) = [\rho_{xy}^{raw}(B) - \rho_{xy}^{raw}(-B)]/2$, where the sweep direction of B is opposite between $\rho_{xy}^{raw}(B)$ and $\rho_{xy}^{raw}(-B)$ to clarify the hysteresis.

We first show the temperature dependence of the longitudinal resistivity (ρ_{xx}) in Fig. 1(a). Those at $B = 0$ T (solid curves) show a clear insulator-to-metal transition accompanied

*Author to whom correspondence should be addressed: kozuka@ap.t.u-tokyo.ac.jp

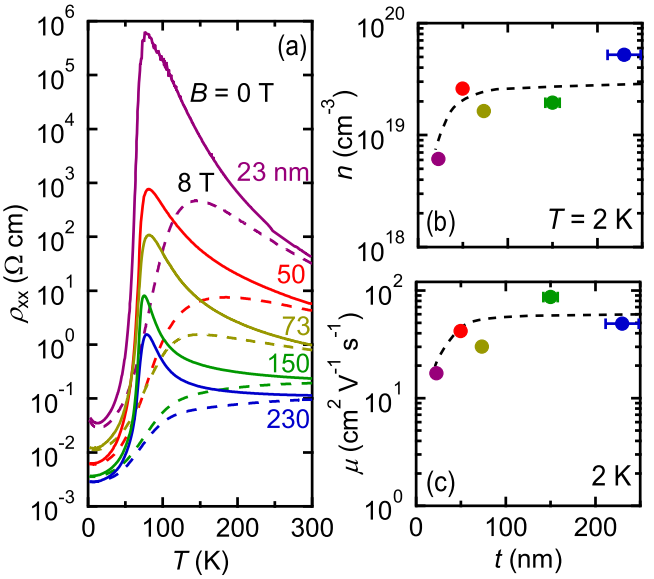

FIG. 1. (Color online) (a) Temperature (T) dependence of resistivity (ρ_{xx}) for EuO films with different film thicknesses (t) at 0 T (solid curve) and 8 T (dashed curve). Film thickness dependence of (b) electron density (n) and (c) mobility (μ) at 2 K. The dashed curves are the guides to the eyes.

with the ferromagnetic transition. Applying a magnetic field of 8 T reduces ρ_{xx} (dotted curves) particularly around T_C, being consistent with those previously reported owing to double exchange–like strong coupling [9,10,13–15]. With increasing the film thickness, ρ_{xx} is slightly but systematically decreased probably due to partial surface depletion as well as carrier scattering at the interfaces of the films. These are verified from thickness dependence of carrier density (n) and electron mobility (μ) as shown in Figs. 1(b) and 1(c).

Next we focus on the Hall effect for these samples. The Hall resistivity (ρ_{xy}) is expressed as

$$\rho_{xy} = R_H B + \rho_{AHE} + \rho_{THE} \quad (1)$$

where R_H is the ordinary Hall coefficient, ρ_{AHE} is the conventional anomalous Hall resistivity proportional to magnetization, and ρ_{THE} is the topological Hall resistivity generated by scalar spin chirality in real space [16,17]. We extract the sum of the anomalous Hall and topological Hall terms by subtracting linear term $R_H B$ from ρ_{xy}, where R_H is estimated in the high field region above 6 T as an example shown in Fig. 2(a) for 30 K. Figures 2(b)–2(f) show $\rho_{AHE} + \rho_{THE}$ for the 50 nm sample at several temperatures below 50 K in the metallic region. As we previously reported in Ref. [10], the sign of ρ_{AHE} above the saturation field is inverted from negative to positive with cooling across ~25 K. In addition to the conventional anomalous Hall term, unconventional peaks emerge from 0 T to 3 T as indicated by the shaded areas. The sign of the peak structure is negative for $B > 0$, which is the same sign as the ordinary Hall term, regardless of the sign of ρ_{AHE}. The peaks are located around 2 T, which corresponds to the onsets of the magnetization inversion (downward sweep, red arrows) or the saturation (upward sweep, blue arrows) for the out-of-plane external magnetic field [9]. This behavior of the peak structures in the Hall effect is reminiscent of THE

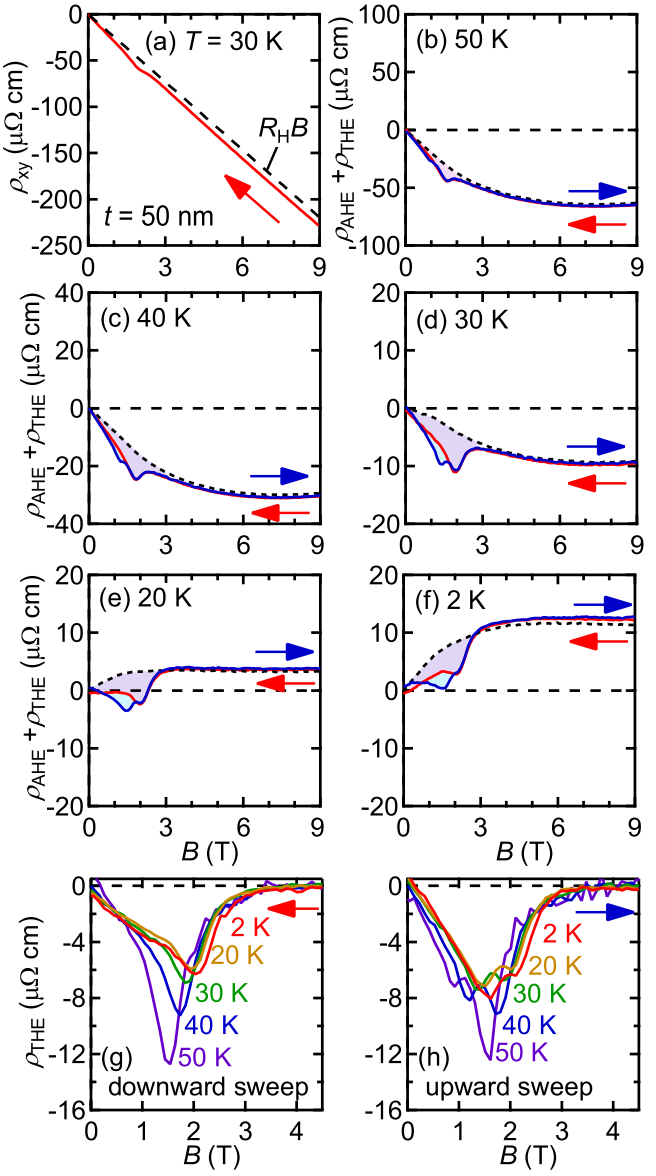

FIG. 2. (Color online) (a) Magnetic field (B) dependence of Hall resistivity for a 50-nm-thick film at 30 K. The broken line is the linear fit to the high-field region to extract the Hall coefficient (R_H). The sum of anomalous and topological Hall resistivities ($\rho_{AHE} + \rho_{THE}$) at (b) 50 K, (c) 40 K, (d) 30 K, (e) 20 K, and (f) 2 K for the 50-nm-thick film. The dotted curves indicate the contribution from AHE that is deduced from the experiments with inclined external magnetic field by 10° as shown in Fig. 3. The shaded areas correspond to the contribution from THE (ρ_{THE}) and the arrows indicate the sweep direction of B. The temperature dependence of ρ_{THE} is shown in (g) for downward and (h) for upward sweeps for perpendicular magnetic field.

caused by magnetic skyrmions. The noise level is one order smaller than the amplitude of the peaks, showing that they are sufficiently distinguishable from electrical noises in all measurements.

There are mainly three types of possible origins to give rise to such an unconventional Hall signal: multicarrier in the ordinary Hall effect, nonmonotonic behavior in the conventional anomalous Hall effect (AHE), and a noncoplanar spin

structure leading to THE. First, the multicarrier contribution can be easily excluded because the conduction band of EuO is composed of one electron pocket at the X point and multicarrier transport has not been reported so far [10,18]. Secondly, nonmonotonic behavior in the conventional AHE could be caused by topologically trivial spin structures such as cone phase through skew scattering process [19,20]. However, we can conjecture that this skew scattering contribution rarely affects the Hall signal observed in EuO thin films in this study, since the conductivity of EuO thin films (1×10^0 S/cm to 5×10^2 S/cm) is in the range of dirty regime ($\sigma_{xx} < 3 \times 10^3$ S/cm), where intrinsic contribution from the Berry curvature of electron wave function is in effect, in contrast to a clean regime where skew scattering is dominant [21]. Therefore, we are tempted to consider topological Hall contribution from the noncoplanar spin structure as the origin of the peak structure in the Hall effect.

While THE is currently perceived as an indication of a noncoplanar spin structure [22], it is still an indirect method to detect the magnetic skyrmions compared with more direct ones by Lorentz transmission electron microscopy [4,5,23,24], magnetic force microscope [25], or neutron scattering [3,26,27]. Nevertheless, THE is widely used and established as an evidence of skyrmions in helimagnetic $B20$-type metallic compounds [6,7,22,28–34]. As a matter of fact, in EuO, the direct microscopy and diffraction methods are not easy since the surface is easily oxidized when it is exposed to air, so that the surface should be covered with an inert film (Al_2O_3 in our samples) to measure intrinsic properties with less magnetic dead layer. Thus THE may be the best way to detect the topologically nontrivial magnetic structures such as magnetic skyrmions for this material at the moment.

In addition to THE in an out-of-plane magnetic field, the existence of magnetic skyrmions or other topologically nontrivial spin configurations is further supported by THE with inclining the sample with respect to the magnetic field. This is based on the destruction of 2D skyrmions due to the limitation of the size of the skyrmion along the thickness direction [Fig. 3(a)]. The angular (θ) dependence of $\rho_{AHE} + \rho_{THE}$ for the 50-nm-thick sample in downward (upward) sweep at 30 K is shown in Fig. 3(b) [Fig. 3(c)], where θ is the angle between the magnetic field and the direction normal to the sample surface [inset of Fig. 3(b)]. The peak structures dramatically decrease with tilting the sample and completely disappear at $\theta = 10°$. The high sensitivity of ρ_{THE} to the tilt angle clearly indicates the formation of 2D magnetic skyrmions or other nontrivial spin structures with a substantially large scale. Also in the case of $Mn_{1-x}Fe_xSi$, for example, THE disappears with increasing the inclination angle of applied magnetic field [34], which agrees with the present observation in EuO thin films.

Besides the peak structures common to both sweep directions marked with filled triangles in Figs. 3(b) and 3(c) (peak 1), another peak (peak 2) is observed only in upward sweeps marked with open squares in Fig. 3(c). Figures 3(d) and 3(e) show the θ dependence of magnetic fields at each peak (B_{peak1} and B_{peak2}) and absolute values of ρ_{THE} at the peaks, respectively. For peak 1, both B_{peak1} and $|\rho_{THE}|$ are independent of the sweep direction and B_{peak1} is almost unchanged until THE disappears at $\theta = 10°$, which is consistent with the reported behavior of 2D skyrmions in $Mn_{1-x}Fe_xSi$ (Ref. [34]). On the other hand, for peak 2, B_{peak2} gradually shifts toward 0 T [Fig. 3(d)] and $|\rho_{THE}|$ vanishes more drastically than that of peak 1 [Fig. 3(e)]. Also, the amplitude of $|\rho_{THE}|$ for peak 2 is independent of temperature in our experimental condition, while that for peak 1 decreases until around 15 K. These properties imply the existence of another type of spin structure with larger size giving peak 2, which may be stabilized depending on the field sweep direction.

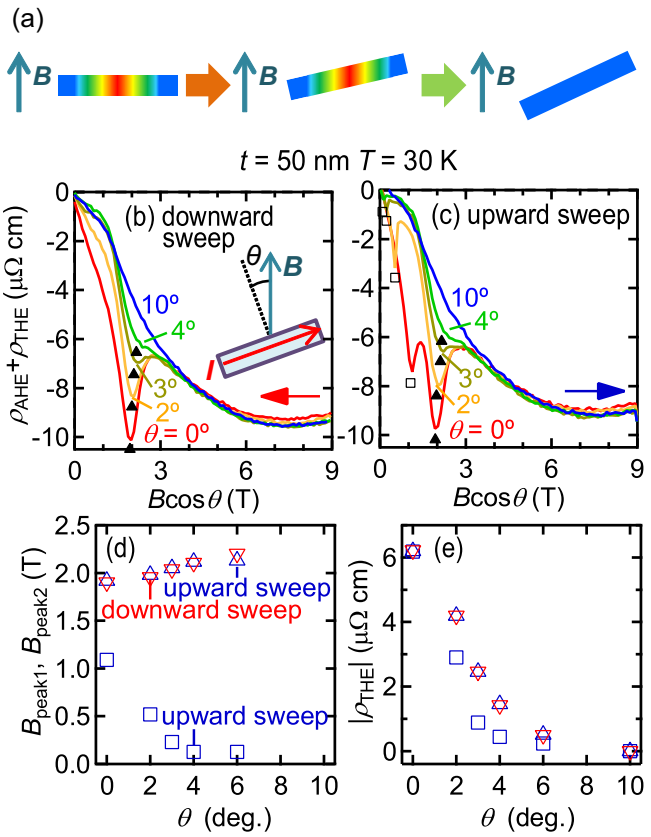

FIG. 3. (Color online) (a) Schematic diagram of a 2D magnetic structure in a film under inclined external magnetic field. Red (blue) corresponds to spin configuration (anti)parallel to magnetic field. The sum of anomalous and topological Hall resistivities ($\rho_{AHE} + \rho_{THE}$) as a function of perpendicular magnetic field ($B\cos\theta$) for (b) downward and (c) upward sweeps of B. Peak 1 (filled triangle) appears in both cases, while peak 2 (open square) does only for upward sweep. The inset of (b) shows the rotation geometry of a sample and current (I). (d) Magnetic fields (B_{peak1}, B_{peak2}) where peaks of THE appear and (e) their absolute amplitudes ($|\rho_{THE}|$) as a function of inclination angle. Down-pointing (up-pointing) open triangles represent the peak 1 in downward (upward) sweep and open squares correspond to the peak 2 in upward sweep.

Now that ρ_{THE} disappears in an inclined magnetic field of 10° with ρ_{AHE} almost intact, we can focus on the detailed temperature dependence of ρ_{THE} as shown in Figs. 2(g) (downward sweep) and 2(h) (upward sweep). We estimate ρ_{THE} at $\theta = 0°$ by subtracting ρ_{AHE} term from Figs. 2(b)–2(f) as $(\rho_{AHE} + \rho_{THE})_{\theta=0°} - S(\rho_{AHE} + \rho_{THE})_{\theta=10°}$, where S is a parameter to give $\rho_{THE} = 0$ at high field and is about 1.05 ± 0.03 in all the temperature range. As shown in these figures, ρ_{THE} decreases with decreasing temperature, and saturates

below 30 K. The magnetic field which gives the maximum of the peak 1 in ρ_{THE} shifts from about 1.6 T at 50 K to 2.0 T at 2 K regardless of the sweep direction, which is qualitatively in agreement with the behavior of skyrmions in $B20$ compounds exhibiting hardening with lowering temperature [5,33].

In spite of the qualitative resemblance of THE between EuO and $B20$-type skyrmion materials such as $Mn_{1-x}Fe_xSi$, the formation mechanism of the magnetic skyrmion is not clear in EuO thin films since there is neither DM interaction nor magnetic frustration, which induces skyrmion phases. One possibility may be related to the interface between the EuO film and the $YAlO_3$ substrate or the surface to cause the four-spin exchange interaction as observed in Fe deposited on Ir (Ref. [35]). However, this scenario is unlikely because the size of magnetic skyrmions induced by this mechanism tends to be small in the atomic scale [1,35] as opposed to the sensitive angle dependence in Fig. 3. As another possibility, it is notable that there is a theoretical proposal of magnetic skyrmion by Belavin and Polyakov (BP) that is based on a simple concept that skyrmion is a topologically nontrivial metastable solution for the classical 2D Heisenberg ferromagnet in the continuous limit [36,37]. However, this model assumes an isotropic ferromagnet in contrast to EuO thin films, which possess in-plane easy axis. Moreover, it is theoretically proved that stationary magnetic skyrmions are unstable in a nonlinear field model [38].

Nevertheless, significance of dimensionality is obtained from the thickness (t) dependence of ρ_{THE}. Figures 4(a) and 4(b) show estimates of the effective magnetic field (B_{eff}) produced by the spin chirality effect and the skyrmion radius (R), respectively, as a function of film thickness. Here, B_{eff} is calculated as $B_{eff} = |\rho_{THE}/R_H|$ at temperatures where $\rho_{AHE} \approx 0$ and R is estimated as $R = t/2 \sin\theta_s$ (θ_S is the angle where THE disappears). As the film becomes thicker than 50 nm, B_{eff} rapidly decreases, reaching zero at $t = 230$ nm, and R diverges. This tendency indicates that the topological spin structure is stabilized only in the 2D limit, phenomenologically in accord with the BP model of magnetic skyrmion in the 2D Heisenberg system. Though B_{eff} also falls off at $t = 23$ nm, this is likely to reflect the effect of magnetic dead layer around the interfaces.

Although the experimental result supports the formation of a 2D topologically nontrivial magnetic structure, the detailed spin structure or its distribution is not clear at the moment. Unlike triangular skyrmion lattices observed in $B20$-type compounds, it is possible that skyrmions with both right- and left-handed twists distribute randomly, since the original theoretical model only considers the existence of a single skyrmion in a 2D Heisenberg ferromagnet as a result of fluctuation-induced metastable state [36,37]. Here, right- and left-handed skyrmions do not compensate THE but give the same sign because of the same topological number [1]. One of the characteristic features of this model is that magnetic skyrmions are fluctuation driven to a metastable state. As shown in Fig. 2, in fact, magnetic skyrmions may be induced under infinitesimal magnetic field as ρ_{THE} increases from 0 T. This behavior is contrasted with the case for $B20$-type compounds, where skyrmions are formed in the limited ranges of magnetic field close to magnetization saturation [28–30].

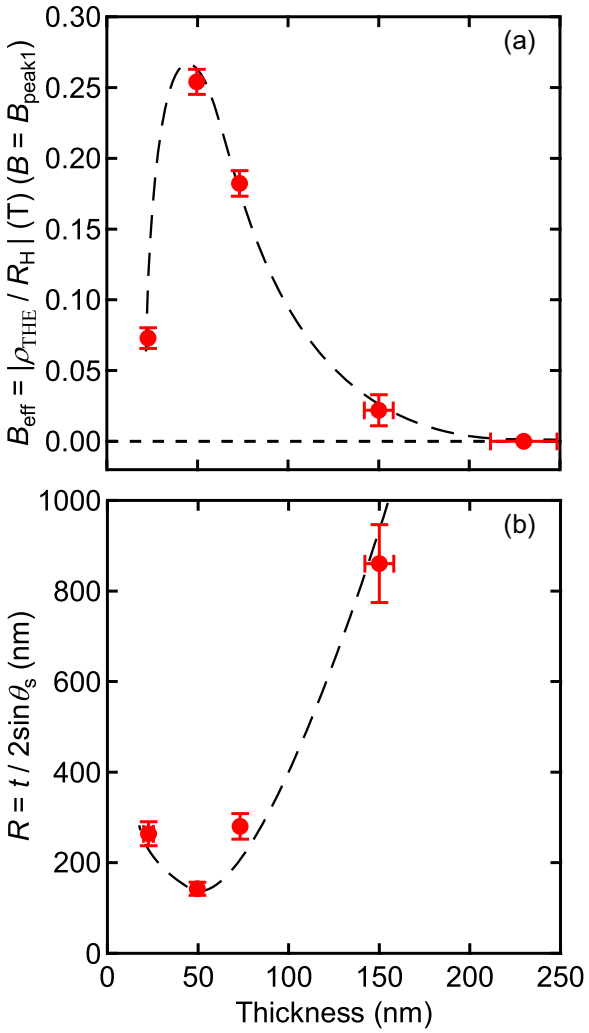

FIG. 4. (Color online) Film-thickness dependence of (a) effective magnetic field ($B_{eff} = |\rho_{THE}/R_H|$) and (b) skyrmion radius ($R = t/2 \sin\theta_s$) at B_{peak1}. The dashed curves are the guides to the eyes.

In the material's aspect, the present study is an observation of THE among magnetic semiconductors. So far, magnetic skyrmions is mostly limited in metallic alloys and in insulators such as Cu_2OSeO_3 (Ref. [22]) and ferrites. In contrast to these materials, semiconductors have an advantage in that the conductivity and carrier density can be modulated by chemical doping, electrostatic doping, or optical irradiation. This property would also have a technological impact in combination with current driving of magnetic skyrmions as information media [39].

In conclusion, we have found unconventional peaks in Hall resistivity reminiscent of THE in a typical Heisenberg ferromagnet EuO only in the thin limit. By inclining applied magnetic field, THE dramatically disappears, suggestive of a 2D topologically nontrivial spin structure. Our observation qualitatively fits the theoretical model predicting magnetic skyrmions in a 2D Heisenberg ferromagnet. This study suggests that magnetic skyrmions are not limited to chiral materials or interfaces but various possibilities of formation mechanisms could be present.

We thank Y. Tokura, Y. Motome, and N. Kanazawa for valuable discussions. This work was partly supported by Japan Society for the Promotion of Science through Program for Leading Graduate Schools (MERIT) and by JSPS Grants-in-Aid for Scientific Research(S) No. 24226002 and Challenging Exploratory Research No. 26610098.

[1] N. Nagaosa and Y. Tokura, Nat. Nanotechnol. **8**, 899 (2013).
[2] U. K. Rößler, A. N. Bogdanov, and C. Pfleiderer, Nature (London) **442**, 797 (2006).
[3] S. Mühlbauer, B. Binz, F. Jonietz, C. Pfleiderer, A. Rosch, A. Neubauer, R. Georgii, and P. Böni, Science **323**, 915 (2009).
[4] X. Z. Yu, Y. Onose, N. Kanazawa, J. H. Park, J. H. Han, Y. Matsui, N. Nagaosa, and Y. Tokura, Nature (London) **465**, 901 (2010).
[5] X. Z. Yu, N. Kanazawa, Y. Onose, K. Kimoto, W. Z. Zhang, S. Ishiwata, Y. Matsui, and Y. Tokura, Nat. Mater. **10**, 106 (2011).
[6] S. Ishiwata, M. Tokunaga, Y. Kaneko, D. Okuyama, Y. Tokunaga, S. Wakimoto, K. Kakurai, T. Arima, Y. Taguchi, and Y. Tokura, Phys. Rev. B **84**, 054427 (2011).
[7] S. Chakraverty, T. Matsuda, H. Wadati, J. Okamoto, Y. Yamasaki, H. Nakao, Y. Murakami, S. Ishiwata, M. Kawasaki, Y. Taguchi, Y. Tokura, and H. Y. Hwang, Phys. Rev. B **88**, 220405(R) (2013).
[8] X. Yu, M. Mostovoy, Y. Tokunaga, W. Zhang, K. Kimoto, Y. Matsui, Y. Kaneko, N. Nagaosa, and Y. Tokura, Proc. Natl. Acad. Sci. U.S.A. **109**, 8856 (2012).
[9] T. Yamasaki, K. Ueno, A. Tsukazaki, T. Fukumura, and M. Kawasaki, Appl. Phys. Lett. **98**, 082116 (2011).
[10] Y. Ohuchi, Y. Kozuka, N. Rezaei, M. S. Bahramy, R. Arita, K. Ueno, A. Tsukazaki, and M. Kawasaki, Phys. Rev. B **89**, 121114(R) (2014).
[11] A. Mauger and C. Godart, Phys. Rep. **141**, 51 (1986).
[12] N. Miyata and B. E. Argyle, Phys. Rev. **157**, 448 (1967).
[13] A. Schmehl, V. Vaithyanathan, A. Herrnberger, S. Thiel, C. Richter, M. Liberati, T. Heeg, M. Röckerath, L. F. Kourkoutis, S. Mühlbauer, P. Boni, D. A. Muller, Y. Barash, J. Schubert, Y. Idzerda, J. Mannhart, and D. G. Schlom, Nat. Mater. **6**, 882 (2007).
[14] M. R. Oliver, J. O. Dimmock, A. L. McWhorter, and T. B. Reed, Phys. Rev. B **5**, 1078 (1972).
[15] Y. Shapira, S. Foner, and T. B. Reed, Phys. Rev. B **8**, 2299 (1973).
[16] N. Nagaosa, J. Sinova, S. Onoda, A. H. MacDonald, and N. P. Ong, Rev. Mod. Phys. **82**, 1539 (2010).
[17] D. Xiao, M. C. Chang, and Q. Niu, Rev. Mod. Phys. **82**, 1959 (2010).
[18] D. E. Shai, A. J. Melville, J. W. Harter, E. J. Monkman, D. W. Shen, A. Schmehl, D. G. Schlom, and K. M. Shen, Phys. Rev. Lett. **108**, 267003 (2012).
[19] T. L. Monchesky, J. C. Loudon, M. D. Robertson, and A. N. Bogdanov, Phys. Rev. Lett. **112**, 059701 (2014).
[20] S. A. Meynell, M. N. Wilson, J. C. Loudon, A. Spitzig, F. N. Rybakov, M. B. Johnson, and T. L. Monchesky, Phys. Rev. B **90**, 224419 (2014).
[21] S. Onoda, N. Sugimoto, and N. Nagaosa, Phys. Rev. B **77**, 165103 (2008).
[22] Y. Taguchi, Y. Oohara, H. Yoshizawa, N. Nagaosa, and Y. Tokura, Science **291**, 2573 (2001).
[23] S. Seki, X. Z. Yu, S. Ishiwata, and Y. Tokura, Science **336**, 198 (2012).
[24] X. Z. Yu, N. Kanazawa, W. Z. Zhang, T. Nagai, T. Hara, K. Kimoto, Y. Matsui, Y. Onose, and Y. Tokura, Nat. Commun. **3**, 988 (2012).
[25] P. Milde, D. Köhler, J. Seidel, L. M. Eng, A. Bauer, A. Chacon, J. Kindervater, S. Mühlbauer, C. Pfleiderer, S. Buhrandt, C. Schütte, and A. Rosch, Science **340**, 1076 (2013).
[26] N. Kanazawa, J.-H. Kim, D. S. Inosov, J. S. White, N. Egetenmeyer, J. L. Gavilano, S. Ishiwata, Y. Onose, T. Arima, B. Keimer, and Y. Tokura, Phys. Rev. B **86**, 134425 (2012).
[27] S. Seki, J. H. Kim, D. S. Inosov, R. Georgii, B. Keimer, S. Ishiwata, and Y. Tokura, Phys. Rev. B **85**, 220406(R) (2012).
[28] T. Schulz, R. Ritz, A. Bauer, M. Halder, M. Wagner, C. Franz, C. Pfleiderer, K. Everschor, M. Garst, and A. Rosch, Nat. Phys. **8**, 301 (2012).
[29] M. Lee, W. Kang, Y. Onose, Y. Tokura, and N. P. Ong, Phys. Rev. Lett. **102**, 186601 (2009).
[30] A. Neubauer, C. Pfleiderer, B. Binz, A. Rosch, R. Ritz, P. G. Niklowitz, and P. Böni, Phys. Rev. Lett. **102**, 186602 (2009).
[31] N. Kanazawa, Y. Onose, T. Arima, D. Okuyama, K. Ohoyama, S. Wakimoto, K. Kakurai, S. Ishiwata, and Y. Tokura, Phys. Rev. Lett. **106**, 156603 (2011).
[32] S. X. Huang and C. L. Chien, Phys. Rev. Lett. **108**, 267201 (2012).
[33] Y. Li, N. Kanazawa, X. Z. Yu, A. Tsukazaki, M. Kawasaki, M. Ichikawa, X. F. Jin, F. Kagawa, and Y. Tokura, Phys. Rev. Lett. **110**, 117202 (2013).
[34] T. Yokouchi, N. Kanazawa, A. Tsukazaki, Y. Kozuka, M. Kawasaki, M. Ichikawa, F. Kagawa, and Y. Tokura, Phys. Rev. B **89**, 064416 (2014).
[35] S. Heinze, K. von Bergmann, M. Menzel, J. Brede, A. Kubetzka, R. Wiesendanger, G. Bihlmayer, and S. Blügel, Nat. Phys. **7**, 713 (2011).
[36] A. A. Belavin and A. M. Polyakov, Pis'ma Zh. Eksp. Teor. Fiz. **22**, 503 (1975) [JETP Lett. **22**, 245 (1975)].
[37] Ar. Abanov and V. L. Pokrovsky, Phys. Rev. B **58**, R8889 (1998).
[38] G. H. Derrick, J. Math. Phys. **5**, 1252 (1964).
[39] J. Iwasaki, M. Mochizuki, and N. Nagaosa, Nat. Commun. **4**, 1463 (2013).